

## Direct Evidence of the Magnetic Properties of $\text{Na}_3\text{Ni}_2\text{SbO}_6$ Nanopowder using X-Ray Magnetic Circular Dichroism

R. DAWN<sup>1</sup>, A. KUMAR<sup>1</sup>, V. K. VERMA<sup>2</sup>, K. KUMAR<sup>3</sup>, A. PRAMANIK<sup>4</sup>, A. KANDASAMI<sup>5</sup> and K. AMEMIYA<sup>6</sup>, V. R. SINGH<sup>1\*</sup>

<sup>1</sup>Department of Physics, Central University of South Bihar, Gaya 824236

<sup>2</sup>Department of Physics, VIT-AP University, Beside AP Secretariat, Near Vijayawada, Amaravati 522237 A.P. India

<sup>3</sup>Department of Physics, Ranchi University, Ranchi 834008, India

<sup>4</sup>School of Physical Sciences, Jawaharlal Nehru University, New Delhi 110067, India

<sup>5</sup>Department of Physics & Centre for Interdisciplinary Research, University of Petroleum and Energy Studies (UPES) Dehradun, Uttarakhand 248007, India

<sup>6</sup>Photon Factory, IMSS, High Energy Accelerator Research Organization, Tsukuba, Ibaraki 305-0801, Japan

1. **INTRODUCTION:** In this era for energy independence and ecological sustainability, honeycomb layered oxides have grown enormous interest for their potential as rechargeable battery components due to their fascinating two-dimensional (2D) ionic diffusion as governed by phase transitions. These compounds generally adopt the chemical composition  $\text{A}_2\text{M}_2\text{DO}_6$ ,  $\text{A}_3\text{M}_2\text{DO}_6$ , or  $\text{A}_4\text{MDO}_6$  (where M can be divalent or trivalent transition metal atoms such as Cr, Mn, Fe, Co, Ni, Cu, or some combination thereof; D represents pentavalent or hexavalent pnictogen or chalcogen metal atoms such as Te, Sb, Bi; and A can be alkali atoms such as Li, Na, K, etc., or coinage-metal atoms such as Cu, Ag, etc.) [1]. Such structures comprise an array of transition metal sheets consisting of  $\text{DO}_6$  octahedra surrounded by multiple  $\text{MO}_6$  octahedra in a distinct hexagonal (honeycomb) alignment. Oxygen atoms from the octahedra in turn coordinate with  $\text{A}^+$  cations interposed between the layers to form heterostructures whose interlayer bonds are significantly weaker than the covalent in-plane bonds. Progress toward their battery application has been hindered by the scarcity of evidence for their unique topologies, nanoscale defects and curvature effects that ought to accompany their otherwise well-reported stacking sequences. Currently, with the rapid increase of lithium-ion battery (LIB) applications in portable devices and electric vehicles, the present lithium resources can hardly meet the growing global demand. To tackle this problem, sodium-ion batteries (NIBs) have been pursued as a promising alternative due to their low cost, abundant supply as well as the

electrochemical similarities to LIBs. Distinct from the common lithium layered oxides, different  $\text{Na}^+$  coordination in prismatic and octahedral site leads to two different types of layered oxides— $P_2$ -type (prismatic) and  $O_3$ -type (octahedral)—and both have been extensively explored as NIB cathode materials [2]. Although  $P_2$ -type cathode materials can deliver a high discharge capacity of more than 190 mAh/g, the low initial Na content and poor cycling stability make them impractical to meet the demands of Na full-cells, therefore,  $O_3$ -type excels  $P_2$ -type due to the sufficient Na content when considered as an ideal  $\text{Na}^+$  reservoir to realize a practical Na-ion battery [3]. The nano-powder with a hope to be capable with such applications that is presented here is  $\text{Na}_3\text{Ni}_2\text{SbO}_6$ , having a chemical composition  $\text{A}_3\text{M}_2\text{DO}_6$ . With this perspective, researchers have tried to introduce  $1/3 \text{ Sb}^{5+}$  cations substitution of  $\text{Ni}^{2+}$  to form the honeycomb-ordered  $\text{NaNi}_{2/3}\text{Sb}_{1/3}\text{O}_2$ . Given the ionic radius and charge difference between  $\text{Ni}^{2+}$  and  $\text{Sb}^{5+}$ , the 2:1 ratio gives rise to a distinct ordered cation arrangement in the  $\text{Ni}_2\text{SbO}_6$  layers where each  $\text{SbO}_6$  octahedron is surrounded by six  $\text{NiO}_6$  octahedrons, forming a honeycomb-ordered superstructure [3]. The partial substitution of Ni by Sb enables the stable low valence state of  $\text{Ni}(+2)$ , inducing an intense electrostatic repulsion between  $\text{Ni}^{2+}$  and  $\text{Sb}^{5+}$  as well as a promoted voltage profile and improved air and thermal stabilities of  $\text{Na}_3\text{Ni}_2\text{SbO}_6$  material [2]. Apart from the so-far studied intrinsic structural disorder in pristine honeycomb-ordered  $\text{Na}_3\text{Ni}_2\text{SbO}_6$  material by means of electron microscopy and associated spectroscopy, it is the very first time tried to explore its electronic

structure and magnetic properties in accordance to discover its physical properties at phase transitions with the help of X-ray Circular Magnetic Dichroism (XMCD) along with X-ray Absorption Spectroscopy (XAS).

2. **EXPERIMENT:** Polycrystalline samples were prepared by the conventional high-temperature solid-state reactions. NiO (Sigma Aldrich,  $\geq 99\%$ ),  $\text{Na}_2\text{NO}_3$  (Rare Metallic (Japan)  $\geq 99.9\%$ ), and  $\text{SbO}_2$  (Sigma Aldrich,  $\geq 99.0\%$ ) were intimately grounded together in an agate mortar to obtain  $\text{Na}_3\text{Ni}_2\text{SbO}_6$ . A 10% excess amount of  $\text{Na}_2\text{NO}_3$  was added to compensate for sodium deficiency susceptible to occur upon annealing at high temperatures and long dwelling time. In order to eliminate any adventitious water,  $\text{Na}_2\text{NO}_3$  was dried overnight at  $100^\circ\text{C}$  before weighing. The nominal mixture was

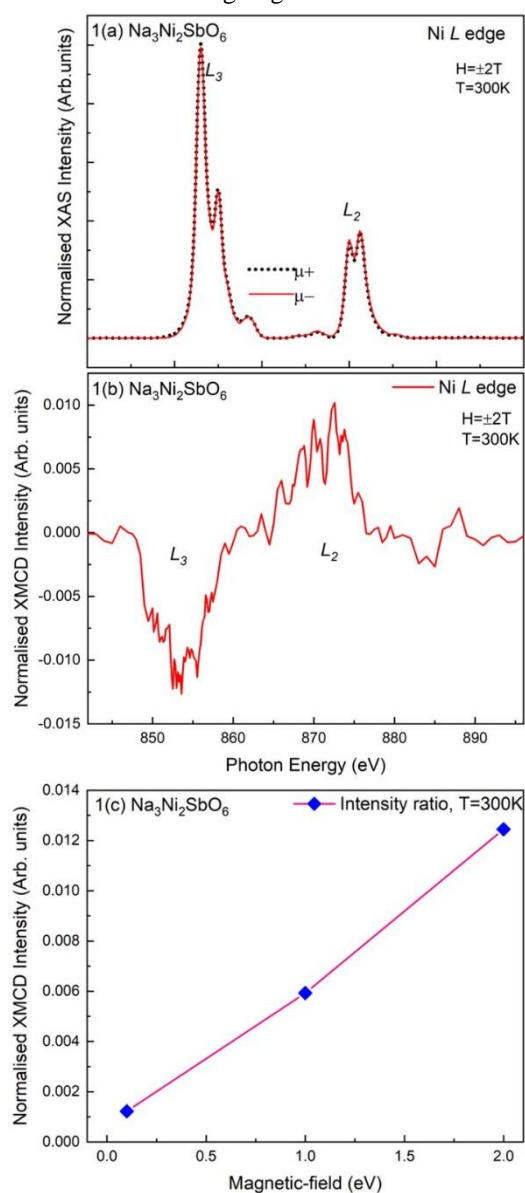


Fig.1: (a) Normalised XAS spectra and (b) normalised XMCD spectra of Ni  $L_{2,3}$  edges of  $\text{Na}_3\text{Ni}_2\text{SbO}_6$  Nano-powder at  $\pm 1.0\text{T}$ , measured at  $300\text{K}$ . Fig. 1(c) represents the XMCD/XAS intensity ratio w.r.t. varying magnetic-field.

then pelletised and heated in Silicon crucibles in air over a duration of 100 hours at  $850 (\pm 5)^\circ\text{C}$  with a heating rate of  $100^\circ\text{C}$  per hour. At the end of the thermal treatment, the furnace was switched off and the samples remained in the furnace during the cooldown. The obtained powders were transferred to an argon-filled glove box, owing to the inherent sensitivity of the materials upon both moisture- and air-exposure.

3. **RESULTS AND DISCUSSIONS:** X-ray spectroscopy, scattering, and imaging experiments were performed at the variable-polarization soft x-ray beam-line BL-16A of the Photon Factory (KEK, Japan). Experimental geometry of soft x-ray absorption (XAS) and x-ray magnetic circular dichroism (XMCD) experiments are shown in Fig. 1. The sample was placed in the vacuum chamber with a pressure of  $10^{-9}$  Torr equipped with a 5 T

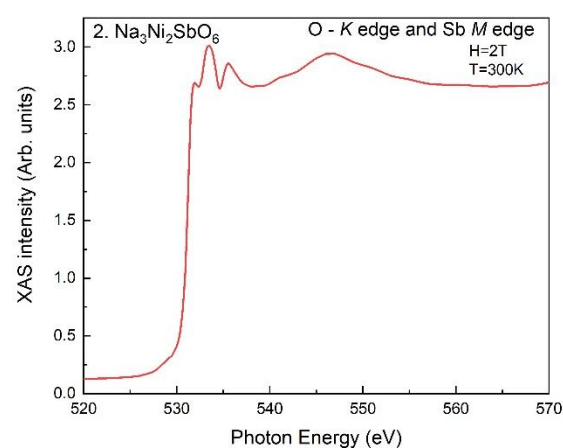


Fig 2: O K edge and Sb  $M_{4,5}$  edge XAS spectra at  $\pm 1.0\text{T}$ , measured at  $300\text{K}$ .

superconducting magnet. XAS and XMCD signals were measured at  $\pm 0.1\text{T}$ ,  $\pm 1\text{T}$  and  $\pm 2\text{T}$  varying magnetic-fields (only the data of  $\pm 1\text{T}$  has been produced here) with right and left circularly polarized (RCP and LCP) x-rays having an energy resolution of  $0.1\text{ eV}$  using the bulk-sensitive total fluorescence yield (TFY) method at Ni  $L_{2,3}$  edges. Sb  $M_{4,5}$  absorption edges is infused with O-K edge due to having same absorption energy range. It has been reported in Werner *et. al.* that  $\text{Na}_3\text{Ni}_2\text{SbO}_6$  possess anti-ferromagnetic phases and a strong temperature dependency exists that yield a tricritical point at Neel Temperature ( $T_N$ ) arising magnetic anisotropy [4]. For this reason, an element dependent spectroscopic study becomes essential to figure out the actual cause of such magnetic behaviour. The XAS spectra obtained with applied magnetic fields of  $+1.0$  and  $-1.0\text{ T}$  are denoted by  $\mu^+$  and  $\mu^-$  which represent left and right circularly polarized light, respectively as shown in Fig 1(a). The XMCD spectrum was recorded by taking a difference between the XAS spectra with negative and positive helicities of the circular

polarized light as shown in Fig 1(b). The Ni absorption peaks shows absorption peak of  $L_3$  with energy  $E = 853.02$  eV arrives with a satellite peak at  $E = 854.97$  eV, whereas,  $L_2$  edge is found to have a multiplet feature at 870.08 eV and 871.35 eV respectively. Some multiplet peaks with lower intensities have been observed at the pre-edge and post edge regions of  $L_2$  and  $L_3$  edge with energy 866.35 and 858.49 eV, respectively verifying the presence of different oxidation states of Ni. This makes sense that the Ni  $2p \rightarrow 3d$  transitions are fairly localized and overlaps with the distorted surrounding atoms. XMCD signal measured in a magnetic field of  $B = \pm 1.0$  T well above the saturation is shown in Fig.1(b) for Ni-edges. Despite that the magnitude of the XMCD measured at the  $L_{2,3}$  edges of Ni, it is clear that the signs of the dichroic signals are almost same. The XMCD/XAS intensity ratio w.r.t. the variable magnetic field with  $\pm 0.1$ T,  $\pm 1.0$ T and  $\pm 2.0$ T (as shown in Fig 1(c)) are found to be increasing with increasing magnetic field, which proves that the Ni present in the  $\text{Na}_3\text{Ni}_2\text{SbO}_6$  gathers a similar magnetic-response w.r.t. the applied magnetic-field.

The presence of Sb  $M_{4,5}$  edges are found to be infused with Oxygen K-edge as shown in Fig 2. We, therefore, observed that the structural disorder is associated with in-plane honeycomb structure and out-of-plane stacking disorder induced by the rotation of  $\text{Na}_3\text{Ni}_2\text{SbO}_6$  layers in the plane. We anticipate that the insight on pristine honeycomb-ordered layered oxides would suggest new clues to researchers exploring the phase transitions occurred in this kind of materials upon cycling and potentially solving their voltage fading and capacity loss issues.

**ACKNOWLEDGEMENTS:** The experiment at the Photon Factory was approved by the Program Advisory Committee (Proposal Nos. 2021G501).

#### References:

- [1] T. Masese, Y. Miyazaki, G. M. Kanyolo, T. Takahashi, M. Ito, H. Senoh and T. Saito, ACS Appl. Nano Mater. **4**, 279–287 (2021).
- [2] L. Xiao, Z. Ding, C. Chen, Q. Huang, P. Gao, W. Wei, iScience **23**, 100898, March, 2020.
- [3] de Boisse, B.M., Cheng, J.H., Carlier, D., Guignard, M., Pan, C.J., Bordere, S., Filimonov, D., Drathen, C., Suard, E., Hwang, B.J., J. Mater. Chem. A **3**, 10976–10989 (2015).
- [4] J. Werner, W. Hergett, J. Park, C. Koo, E.A. Zvereva, A.N. Vasiliev, R. Klingeler, Jour. M. M. M. **481**, 100-103 (2019).